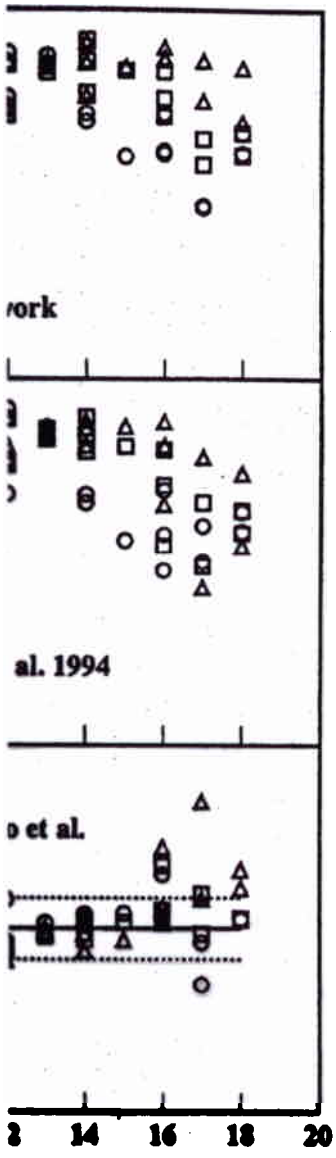

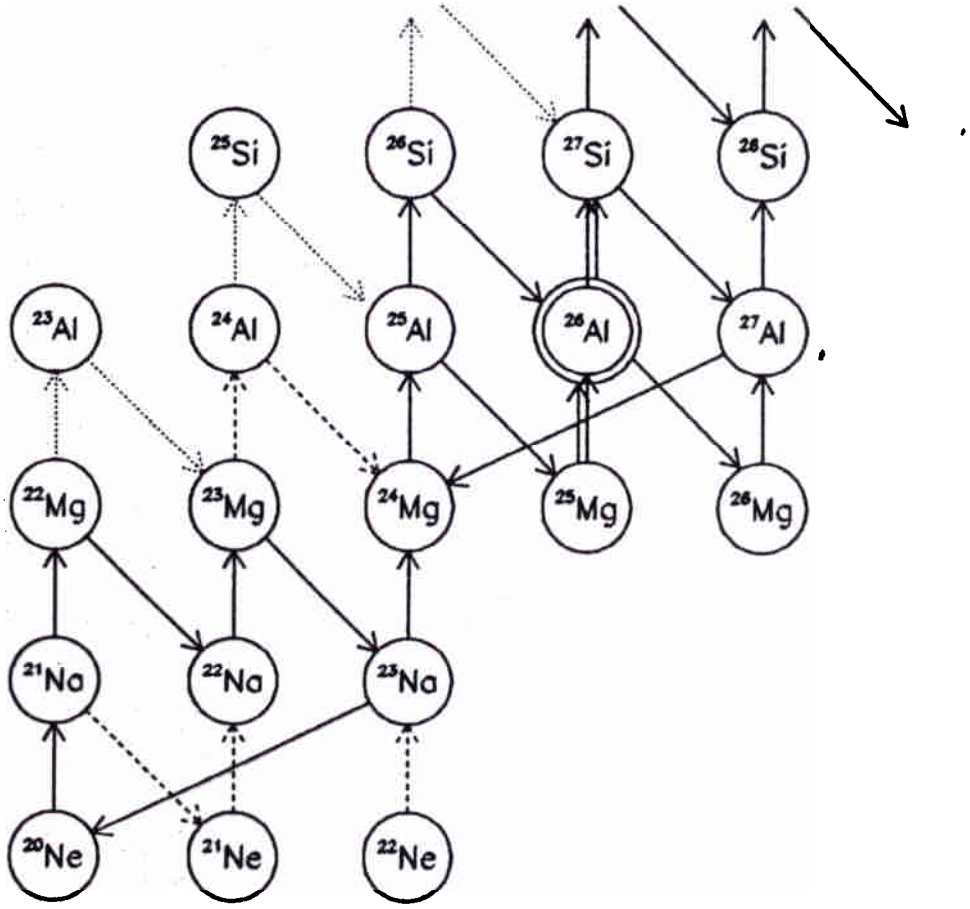

Fig. 4. Nuclear network in the region of interest. The solid, dashed, dotted lines represent the main nuclear flow in order of decreasing intensity (over 5 orders of magnitude). These flows have been integrated over the duration of the outburst in the 1.25 $M_\odot$ case. The ^{26}Al isotope is represented by two circles, the inner one corresponds to the ground state and the outer one to the isomer

Z

figure shows the final
er for the 34 long-lived
ares and triangle corre-
1.25 and 1.35 $M_\odot$) of
of our calculations, the
n is the ratio of the two
with those of PSTWS to
wo dotted lines)

$+ 41.92\, T_9^{1/3}$)

this rate is composed of three terms. The first term, dominant at low temperature ($T_9 \leq 0.1$), is obtained through a Hauser-Feschbach type calculation attempting to take into account the contribution of unknown near-threshold levels in ^{27}Si. The second term gives the contribution of the narrow resonance at E_p = 0.277 MeV whose energy and strength have been carefully measured by Buchmann et al. (1984). The third term is a high-energy continuum rate describing the contribution of known higher-lying resonances (Buchmann et al. 1984). Since CF88, new experimental data appeared concerning the low-energy re-

Vog96 = ^{26}Al(^{3}He, d)^{27}Si;
Wan89 = ^{27}Al(^{3}He, t)^{27}Si;

E_x (^{27}Si) (keV)	E_R (keV)	adopted $\omega\gamma$ (meV)	J^π	Γ (keV)	source
7468	4	1.5 x 10^{-75}			SM Cha93
7532	68	2.2 x 10^{-11}			SM Cha93
7557	93	5.3 x 10^{-9}			SM Cha93
7592	128	5.9 x 10^{-7}			EX Vog96
7652	188	0.064 (for 4)			EX Vog96
7691?	226	?			EX Wan89
7702	238	4.7 x 10^{-3}			SM Cha93
7741	276	3.8 ± 1.0	(9/2,11/2)+	< 0.3	EX Buc84
7792	328	0.2 +0.02-0.01			SM Cha93
7828	363	65 ± 18	(9/2,11/2)+	< 1.0	EX Buc84
8158	693	51 ± 27		< 0.5	EX Buc84
8166	701	16 ± 6		< 0.5	EX Buc84
8227	762	36 ± 13		< 0.5	EX Buc84
8290	825	41 ± 16		< 1.0	EX Buc94
8359	894	67 ± 28		< 0.5	EX Buc94

Table 1 Excitation energies in ^{27}Si and the corresponding ^{26}Al^g+p centre-of-mass resonance energies, adopted resonance strengths and assigned spin-parities and/or total widths; as tabulated in the NACRE compilation [Ang99].

between these mirror nuclei were made, and the maximum level shift was found to be of the order -650 keV.

The current updated knowledge of states in ^{27}Si is represented in figure 1.2. Shown are the Gamow windows for peak temperatures of T_9=0.05, 0.1, 0.2 and 0.3, for both ground state and isomeric state capture. It can be seen from a comparison of the figure and table 1 that there are several states known in ^{27}Si in the region corresponding to low-temperature burning of ^{26}Al^m for which spin-parities and resonance strengths are unknown. The 5^+ ground state of ^{26}Al forms states in ^{27}Si with comparatively large angular momenta: s-wave resonances will form states with J^π=$9/2^+$,$11/2^+$. However the 0+ isomeric state will form states of much lower angular momentum, and indeed can only form states with J^π=$1/2^+$ via s-wave capture. Thus the presence of a state with low angular momentum in the region between 7828 keV < E_x < 8158 keV could facilitate the ^{26}Al^m(p,γ)^{27}Si reaction via s-, p- or d-wave capture.

Looking at the analogue states in ^{27}Al in the region around 8 MeV, it can be seen that there are several candidates with low angular momentum which could correspond to some of the unassigned states in ^{27}Si. Most striking is the $1/2^+$ state at 8130 keV, which, following the trends in level shifts proposed by Champagne et al., could correspond to one of the five states between 7828 keV and 8158 keV in ^{27}Si and therefore provide a strong s-wave resonance in ^{26}Al^m+p. Also present are the $3/2^-$ state at 8182 keV, which could correspond to an ℓ=1 resonance, and the 5/2 states at 8097 keV and 8136 keV which could correspond to ℓ=2 resonances.

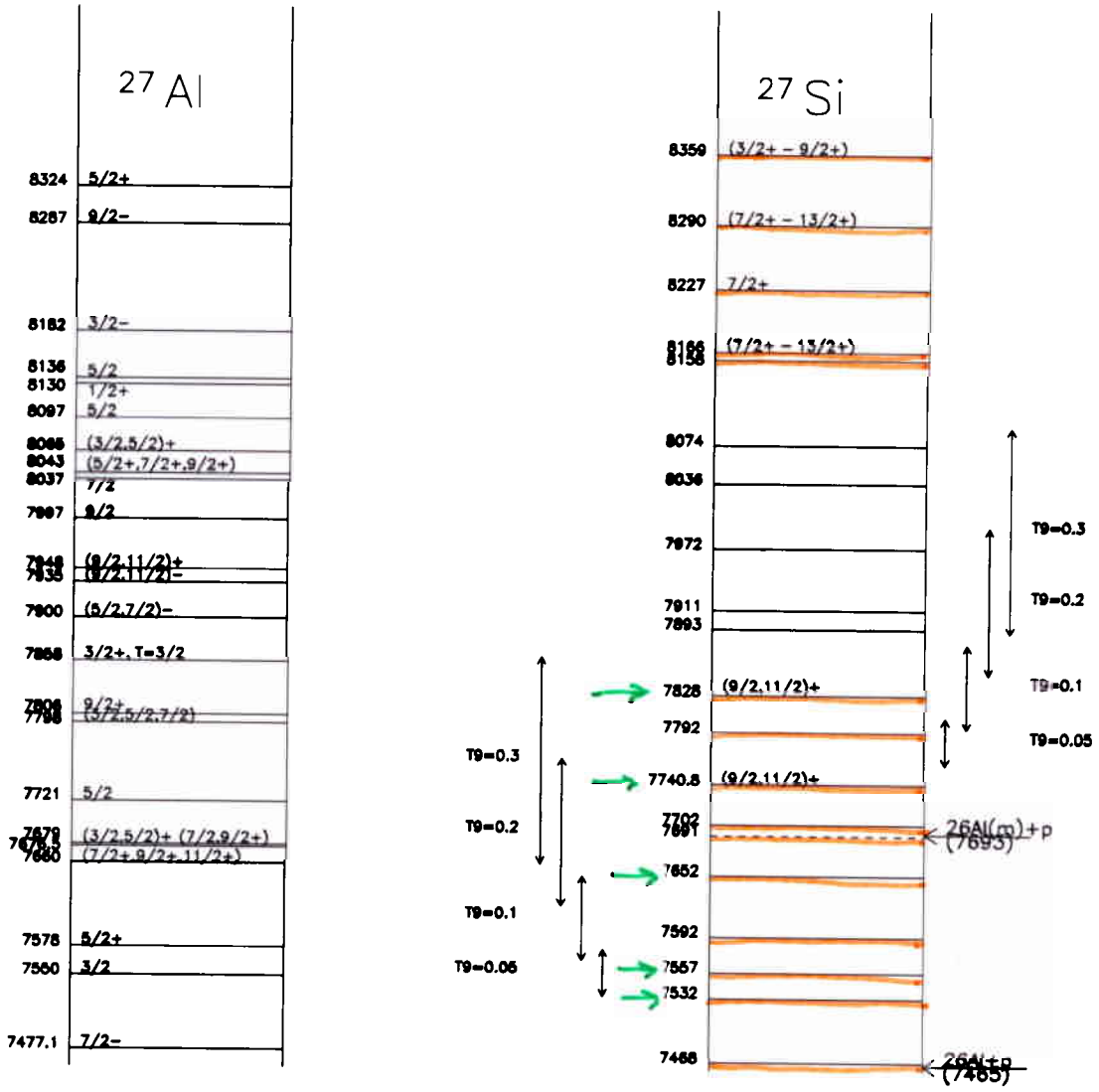

Fig. 1 Comparison of known states in the A=27 analogue system. Marked are the proton-capture thresholds for both $^{26}Al^{g}$ and $^{26}Al^{m}$. Also marked are the Gamow windows for a range of peak temperatures corresponding to both these captures. Data taken from [Ang00] and [End90].

1.3 Resonance Strengths in $^{26}Al^{m}$+p

The possible existence of s-, p- or d-wave resonances in $^{26}Al^{m}$+p introduces the need for the experimental determination of the resonance strengths in order to determine the contribution to the $^{26}Al^{m}(p,\gamma)$ reaction rate, and the subsequent astrophysical consequences. In order to determine the feasibility of measurement of these resonance strengths, and estimate the possible magnitude of their influence, one can derive similar upper limits on resonance strengths as considered for $^{26}Al^{g}$+p in previous work, using the following method. The resonance strength is defined as

$$\omega\gamma = \frac{(2J+1)}{(2I_1+1)(2I_2+1)} \times \frac{\Gamma_\gamma \Gamma_p}{\Gamma_\gamma + \Gamma_p} \tag{1}$$

which for small Γ_γ leads to the approximation $\omega\gamma \approx \omega\Gamma_p$. The upper limit of the resonance strength for different possible ℓ-values can then be calculated by setting the dimensionless proton width, θ_p to unity:

$$\omega\gamma = \omega\frac{3\hbar^2}{\mu r^2} P_\ell(E)\theta_p^2 \tag{2}$$

Table 1.3 shows the resulting maximum resonance strengths assuming s-wave capture, for the ^{27}Si states at 7792 keV and above, up to the 8158 keV state. The state at 7741 keV (E_{cm}=47 keV) has been omitted because of its high spin, while the state at 7702 keV (E_{cm}=10 keV) has been omitted due to an extremely small estimated maximum resonance strength.

Figure 1.3 shows the maximum possible $^{26}Al^{m}(p,\gamma)^{27}Si$ reaction rate contributions from individual resonances assuming s-wave capture, using the resonance strengths from table 1.3. The black curves show the adopted NACRE rate for $^{26}Al^{g}(p,\gamma)^{27}Si$ with upper and lower limits. In the NACRE compilation, the isomeric state rate, $N_A < \sigma v >$, is equal to the ground state rate at low temperatures up until T = 0.11 GK, and exceeds the ground state rate by roughly a factor 4 at T = 0.4 GK. It can be seen that there are a number of possible resonances, which if possesing a resonance strength close to the maximum value based on penetrability arguments, would contribute to the reaction rate causing it to exceed the current adopted rate roughly by between a factor 10 and 500 at temperatures around T = 0.35 GK.

The dominating resonances in this scheme would be those at 200, 218, 279, 343 and 381 keV, the others making no significant contribution to the adopted rate due to either their high energy or small maximum strength. It is then these mid-range resonances that must be measured in order to determine which, if any, are s-wave captures that may be significant to ^{26}Al burning at higher mass nova temperatures.

E_x (keV)	E_R^m (keV)	$\omega\gamma$ ℓ=0,1,2 (meV)
7792	100	0.00018
		3.6e-5
		3.8e-6
7828	135	0.047
		0.01
		0.009
7893	200	21.6
		4.6
		0.5
7911	218	70.7
		15.3
		1.8
7972	279	1.6 eV
		0.4 eV
		0.04 eV
8036	343	16 eV
		3.7 eV
		0.4 eV
8074	381	48 eV
		11 eV
		1.5 eV
8158	465	319 eV
		76 eV
		11 eV

Table 2 Maximum strengths calculated for possible resonances in $^{26}Al^m$+p for ℓ=0,1,2 using a dimensionless proton width equal to unity.

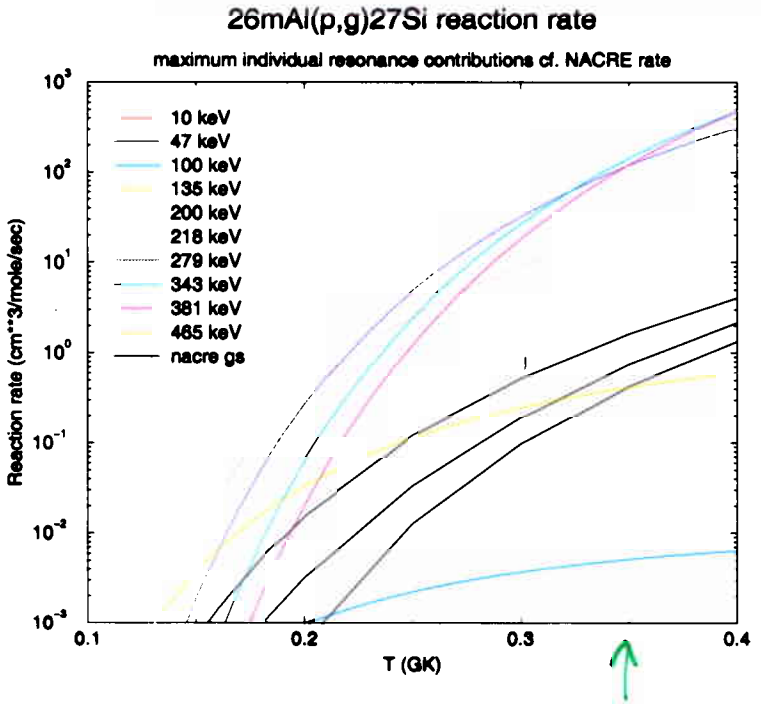

Fig. 2

1-35 $M_\odot$ WD

2 Description of the Experiment

3 Experimental Equipment

4 Readiness

5 Beam Time required

6 Data Analysis